Ocean Engineering 130 (2017) 336–350

Contents lists available at ScienceDirect

Ocean Engineering

journal homepage: www.elsevier.com/locate/oceaneng

Autonomous detection, following and mapping of an underwater chain using sonar

Natàlia Hurtós*, Narcís Palomeras, Arnau Carrera, Marc Carreras

Computer Vision and Robotics Group (VICOROB), University of Girona, 17071 Girona, Spain

ARTICLE INFO

Keywords:
Mooring chain
Autonomous underwater vehicle
Sonar

ABSTRACT

Following an underwater chain using an autonomous vehicle can be a first step towards more efficient solutions for cleaning and inspecting mooring chains. We propose to use sonar as a primary perception sensor to enable the vehicle operation in limited visibility conditions and overcome the possible turbidity arising during marine growth removal. Despite its advantages, working with acoustic data raises additional challenges for the processing and control methodologies involved. We present two chain link detectors that make use of forward-looking sonar and multibeam data and we combine them with adequate planning and control strategies to achieve a robust framework to detect, follow and map an underwater chain. Experiments conducted in a water tank and in a real harbor environment demonstrate the capability of autonomously detecting and following a chain with sufficient accuracy to perform subsequent cleaning or inspection tasks. Besides this, we demonstrate the possibility of obtaining a preliminary map of the chain and its surroundings regardless of visibility conditions.

1. Introduction

Autonomy is a central aspect in the marine robotics community. The present work is framed in the context of the PANDORA European FP7 project (PANDORA, 2016), which aims to increase the range and complexity of underwater tasks that can be automated while reducing the need for operator supervision. To this end, one of the three core tasks of the PANDORA project is to work towards a cost and time efficient solution for the cleaning and inspection of mooring chains using an autonomous underwater vehicle (AUV).

Chain moorings on floating structures such as floating production, storage and offloading (FPSO) vessels are exposed to severe environmental and structural conditions. In order to avoid potential damage, chain status is monitored through periodic and exhaustive inspections. Traditional methods, which involve recovering the chain on deck or ashore, are being replaced by *in situ* in-water inspections using remotely-operated vehicles (ROVs) equipped with mechanical or optical callipers (Welaptega Marine Limited, 2016; Hall, 2005; Morandini and Legerstee,) or chain crawler vehicles (Reece Innovation, 2016). Recent tests have also shown preliminary results in performing a 3D laser scanner inspection from an AUV (Reeves et al., 2014). However, most available solutions require prior removal of the marine biofouling so that the chain can be properly examined. Cleaning solutions range from manual brushing with divers, which is potentially hazardous and has an inherent depth limit, to high-pressure water systems deployed with ROVs (Noble Denton Europe Limited, 2006). The time spent to clean depends strongly on the selected option, but in general is a tedious and slow task since optical visibility drops drastically as the removed marine growth floats in the water. Indeed, considering the cost of ROV vessels, chain cleaning can be a significant fraction of the cost of a chain inspection program (Noble Denton Europe Limited, 2006).

To avoid the presence of troublesome ROV cables and reduce the cost of the deploying vessel, the PANDORA project aims to demonstrate the feasibility of using an AUV equipped with a water jet to conduct chain cleaning and inspection tasks. Such a system could be useful as well in the cleaning and inspection of mooring buoy chains or in general to any large vessel anchor chain (see Fig. 1). Our proposal is to use an AUV with a high resolution imaging sonar (Aris explorer, 3000, 2016), which delivers acoustic images at near-video frame rate, in order to autonomously navigate along the chain and detect each of the links. In this way the cleaning process can be carried out regardless of the visibility conditions and the suspended marine fouling, thus speeding up the overall operation.

Moreover, by mosaicing the sonar images gathered along the chain trajectory, the same methodology provides the means to perform an initial visual inspection, from which it is possible to identify some major issues or locate problematic parts that need further cleaning or

* Corresponding author.
E-mail addresses: nhurtos@eia.udg.edu (N. Hurtós), npalomer@eia.udg.edu (N. Palomeras), acarrera@eia.udg.edu (A. Carrera), marc.carreras@udg.edu (M. Carreras).

http://dx.doi.org/10.1016/j.oceaneng.2016.11.072
Received 17 May 2016; Received in revised form 22 October 2016; Accepted 30 November 2016
Available online 12 December 2016
0029-8018/ © 2016 Elsevier Ltd. All rights reserved.

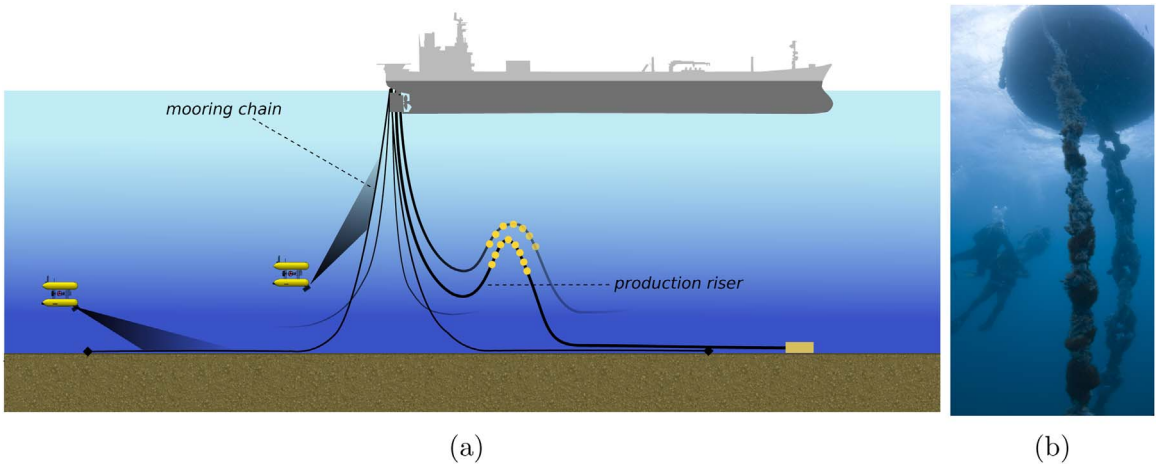

Fig. 1. Potential applications of the proposed system: (a) FPSO mooring lines, (b) buoy moorings and, in general, any scenario where underwater *in situ* chain cleaning and inspection is required.

inspection.

Despite these advantages, the use of such a system produces several challenges that must be addressed. First, the automatic detection of the chain links in forward-looking sonar (FLS) images becomes a complex problem, due to the inherent sonar characteristics: noise, low resolution, moving shadows and intensity variations due to different vantage points. Besides, the control of the AUV must be adapted to take into account the imaging geometry of the FLS, which insonifies a fan-shaped 3D portion of the environment and maps it into a 2D representation. Moreover, the vehicle location at a given instant differs from the point that is being inspected, which is a few meters ahead depending on the sonar's range configuration. Therefore, to successfully follow the chain, the detection and control schemes must be tightly coupled so that the chain links do not drop off the sonar's narrow field of view and the vehicle keeps always track of the chain.

This paper proposes a framework to deal with such challenges, thus providing a solution for the autonomous detection, following and mapping of an underwater chain as a first step towards performing chain cleaning and inspection in a completely automated way.

Our mission scenario consists in an AUV that is deployed in the vicinity of a mooring chain. The presented methodology considers a chain lying approximately on a plane, either horizontal or vertical. Note though, that this approach could be extended to other configurations with the aid of a pan-and-tilt unit in order to set the imaging sonar to the appropriate grazing angle to image the scene. For instance, this would be convenient to address the transition portion of a mooring chain from horizontal to vertical. However, to start with, and given that most part of a mooring chain is either lying on the sea floor or suspended in the water column, the present work focuses in solving the problem in two independent scenarios: horizontal and vertical chain configurations. Even though we assume that the position of the chain in the environment is approximately known, it might not be always possible or practical to deploy the AUV in a location where the chain is readily visible by the sonar systems. Therefore, we must account for a detection phase, in which the vehicle automatically finds the chain in the environment, leading to the following maneuver through the different links, and finally the mapping, which is performed offline using the gathered data. In this paper we propose a framework to address all these phases focusing on the two mentioned scenarios (horizontal and vertical), and thus demonstrate the feasibility of autonomous operations in chain moorings. It is worth underlining here that the details of a possible cleaning system, by means of a water jet integrated on the AUV, fall beyond the scope of this paper.

This paper builds on previous work of the authors. A first offline version of the forward-looking sonar chain link detector was presented in Hurtós et al. (2013). A second version, already running online, was presented in Hurtos et al. (2014), together with a preliminary framework for chain following with the chain in horizontal configuration, which was demonstrated in a water tank. However, the framework presented in this paper has significant improvements, including a whole new trajectory planner module. Moreover, aside from the chain following in the horizontal scenario, we extend and complete the framework by including a new algorithm for dealing with the chain detection and following in the vertical configuration. Furthermore, experiments for both scenarios in a harbor environment have been conducted, reporting results from a more realistic setup.

The reminder of this document is organized as follows. Section 2 describes the proposed solution for detecting and following a chain in horizontal configuration. This includes the proposal of a detection algorithm developed to robustly detect chain links on sonar imagery, the generation of position waypoints from the link detections and the control system of the AUV. Section 3 describes the variations made to this approach in order to tackle the problem for the chain in vertical configuration, which includes the use of an auxiliary multibeam sensor to facilitate the detection and following in the water column. Experiments and results are reported in Section 4, showing the performance of the proposed framework in tests conducted both in a water tank and at sea. Furthermore, we prove the capability of the system to perform mapping with the gathered data by reporting some of the maps generated after the chain following procedures. Finally, Section 5 concludes the paper and points out future work.

2. Horizontal chain detection and following

Throughout this section we consider a mooring chain lying on the seabed. In this scenario, the vehicle navigates at a constant altitude from the seafloor and the FLS tilt angle is set at a small grazing angle (~15° from the horizontal plane) in order to maximize the coverage of the imaged area (see Fig. 2).

Fig. 3 outlines the developed chain-following framework. As the vehicle navigates, the stream of sonar images is processed by a link

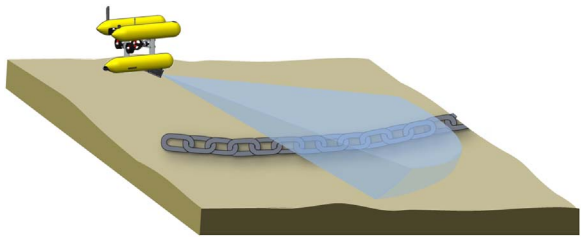

Fig. 2. Chain horizontal scenario.

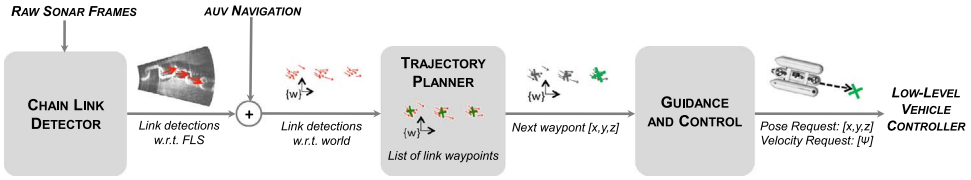

Fig. 3. Diagram illustrating the different steps of the chain following framework for the horizontal scenario.

detection module that identifies the presence of a chain link within the sonar's field of view and delivers its position with respect to the sonar's origin. Notice that our aim is not only to identify the presence and direction of the chain but to detect each of the links as accurately as possible. This will ensure a fitted trajectory over the actual links which is required for cleaning or inspection purposes.

By taking into account the sonar position in the vehicle and the vehicle location in the world coordinate frame, link detections provided by the detection module are referenced with respect to the world coordinate frame. The multiple detections are grouped and associated to the corresponding chain links by a second module, named the trajectory planner. This module maintains a list of all detected links and generates an ordered sequence of waypoints that have to be visited in order to correctly follow the chain.

Finally, a third module implements a combined control system which guides the vehicle towards each waypoint in the sequence while keeping the vehicle orientation facing the last detected link. In this way, the vehicle visits the links that have already been identified while new ones are simultaneously detected and added to the list. This process is executed until the vehicle has reached the position of the last detected link and no link remains unvisited.

Next sections describe each of the involved modules in more detail.

2.1. Detection of chain links on FLS imagery

Although the resolution of new FLS devices is progressively increasing, the inherent characteristics of the acoustic images pose a challenge to the object detection techniques that are typically used on optical images. For instance, the low degree of repeatability when extracting point features in sonar images (Hurtos et al., 2013) leads to unfeasible detection approaches that involve matching features against a visual vocabulary of an object, which is a technique commonly used on video-based object recognition.

FLSs are mainly used to perform inspections from ROVs with a human monitoring the data in real-time, however, there are few examples of the use of FLS devices to perform automatic object detection. Handegard and Williams (2008) have presented an automatic tracking of fish populations in which multiple fishes are detected by applying a sequence of image de-noising filters followed by an intensity thresholding. Xie et al. (2012) demonstrated the detection of underwater pipelines from FLS images, using a Gabor filter and a contour segmentation to detect the elongated perimeter of the pipe. In the context of AUV obstacle detection and path planning Petillot et al. (2001) used an offline two-stage filtering and segmentation scheme with an adaptive thresholding, while Quidu et al. (2012) detected the potential objects in front of the AUV by identifying statistical deviations in small patches of the image. The work of Galceran et al. (2012), focusing on the detection of mine-like targets on the seafloor, is perhaps the most similar to the problem addressed here in the sense that the objects to be detected are well-known beforehand. They take advantage of the integral image representation to locate echo highlights (by subtracting a background map) and then filter them according to the *a priori* known morphology of the object. Later, Ferreira et al. (2014) used the same method but in this case applied to a de-noised image obtained from blending several sonar frames according to their navigation positions. Aside from these examples on FLS data, other works on imaging sonar object detection (i.e., performed with sidescan sonar or mechanically scanning imaging sonars), have also as a common practice employed the segmentation of highlighted areas (either intensity or edge-driven) and the use of shadow cues (Reed et al., 2004; Sawas et al., 2010).

However, given that chain links are not isolated objects but interlaced elements, it is difficult to exploit the use of shadows or intensity thresholds as the individual links cannot be distinctly identified. Likewise, gradient-based or edge-based techniques become unreliable as depending on the link's position there is a wide range of different outcomes in image intensities. There are many possible intensity transitions (from link to background, link to shadow, link to link, shadow to background) together with possible sonar artifacts (e.g., cross-talk or strong reflections) that can contribute to fragmenting and cluttering an edge map, thus complicating the task of identifying the link's contour.

Images in Table 1 exemplify these difficulties. On the top row we can see the result of commonly used methodologies for object detection in sonar images when looking for an isolated target. Leaving aside possible tuning of their parameters, it can be seen that they clearly set a basis for detecting either a shadow, a contour or an echo that can be used for identification. From these outputs, outlier detections could be later discarded by using knowledge of the target (area, shape, etc). However, if we apply the same methodologies over a chain image (bottom row) we obtain cluttered detection maps, where even if we try to impose constraints on size or shape it is impossible to discern if we are really imaging a chain link and, even more challenging, determine accurately the position of each of them.

The detection method proposed here relies mainly on the intensities backscattered by the link itself, which are most of the times under partial occlusions due to the imaging viewpoint or actual objects occluding parts of the chain link, such as other links, shadows, or marine growth. We have approached the problem as a pattern-matching using normalized cross-correlation of local templates, which allows us to detect portions of the link while others are not visible. Those detections are then robustly clustered and related according to their known dimensions and spatial location so as to finally identify the presence of a link and provide an estimation of its center and orientation. Fig. 4 summarizes the link detection process, consisting of the following steps:

- **Image enhancement:** Instead of performing the detection on a raw frame, the system takes advantage of the sonar's high frame rate and registers a small number of n consecutive frames to produce an intermediate image of increased signal to noise ratio (SNR). The registration between frames is performed using Fourier-based techniques (Hurtós et al., 2015) and the resulting image is formed by averaging the intensities at each point thus reducing the noise and the incidence of spurious artifacts present in the individual frames.
- **Pattern matching:** The image generated in the previous step is the basis for performing cross-correlation with local templates, each one rotated into a few different orientations. These templates have been previously defined according to the morphology of the particular chain that has to be followed (e.g, for a studless chain a good template set would be composed of the four link corners and the straight side). Although many links might be present in one image, and therefore several areas can reflect a high correlation response

Table 1
Detection on isolated object vs. chain image.

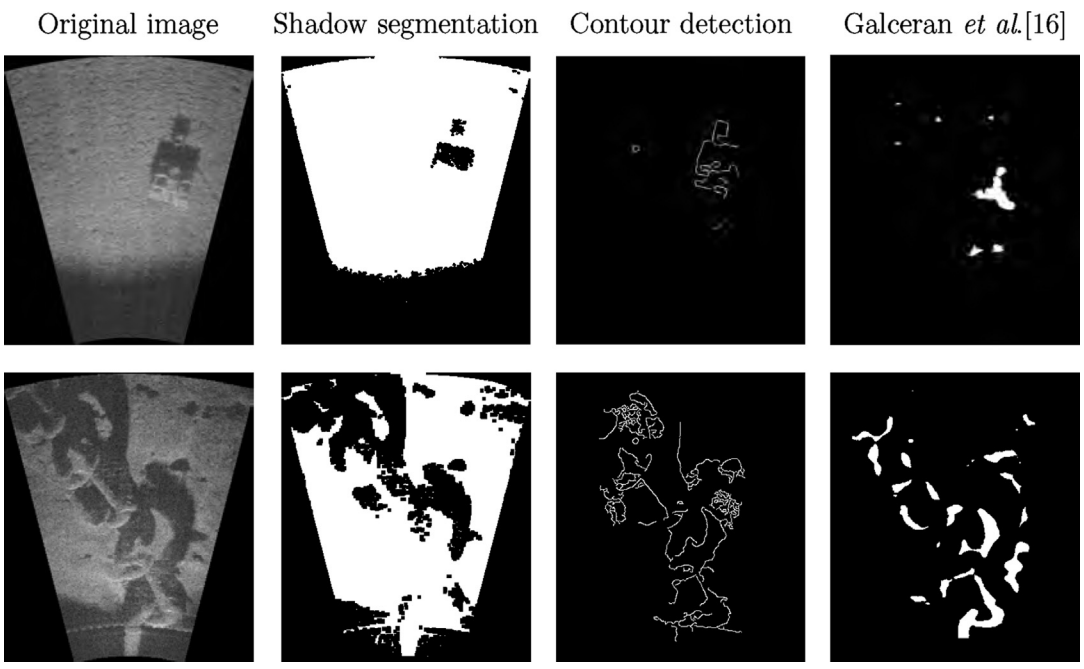

for a given template, only the strongest location for each template is saved.

- **Grouping of template detections:** To increase robustness and discard outliers, template detections are accumulated along several images, according to the displacements identified by registration. If a minimum number of the same template type detections are located within a neighborhood, the detection of that link part is considered valid.
- **Link identification:** Detections of different link parts must be associated into groups belonging to the same link. To that end, we make use of a heuristic that explores a sequence of possibilities according to the detection's spatial location and known link dimensions. Due to link interlacing, alternate links have different inclinations with respect to the main chain axis, making link elements on one side easier to be seen in a given image. Therefore the heuristic sweeps the image for the combination or sub-combination of link elements on the same side (i.e., [lower-left corner/straight segment/upper-left corner] or [lower-right corner/straight segment/upper-right corner]).
- **Orientation estimation:** Once the links have been identified, orthogonal regression is used to fit a line through the detections composing the different groups of a link. The orientation of the fitted line serves as an estimate of the link's orientation.
- **Center estimation:** Finally, using the estimated angle the location of the link's center can be estimated by projecting the known link dimensions from each detection point, assuming a 2D projection.

The most time consuming process of the detection module is the generation of the enhanced image, taking an average of 17 ms per registered frame (for frames smaller than 512×512 pixels) on a Intel Core i7 CPU at 2.2 Mhz. On the same system, the template matching process takes an average of 14 ms given a 32×32 pixels template and a sonar image of 350×497 pixels. However, note that as the detector must be able to work online, the time that it takes to output the detection will be ultimately determined based on a number of factors: the incoming frame rate of the sonar images, the number of frames that are accumulated to generate the enhanced image and the template detections that are accumulated before trying to identify links. The more frames, the more robust will be the detection but less detections will be outputted.

2.2. Chain-follow trajectory planning

As the vehicle moves, the same link might be observed and detected multiple times through the module presented in previous section. However, these estimations can vary around the actual chain link center due to mainly two reasons. On the one hand, the locations found in the template matching step can slightly differ from one observation to the other as the image's intensities fluctuate due to small viewpoint changes. Therefore, the detected location of a part of a link may be slightly different and hence also the final center estimation. Moreover, since the detections are referenced in a world map by using the position of the vehicle, the navigation drift between two detections may cause a slight divergence in their positions. In view of that, we developed a module that: i) classifies the different estimations of the centres into clusters belonging to the same chain link and ii) sorts the clusters in order to request to the vehicle the next way point that needs to be reached to follow the chain.

- **Clustering of link detections:** Scattered link detections are clustered using the mean shift algorithm (Comaniciu and Meer, 2002). Mean shift is an iterative centroid-based algorithm, that updates candidates for cluster centroids according to the mean of the features (in our case detections) within a given region. This is advantageous as it does not require us to know before-hand the present number of clusters (i.e., how many different links have been detected so far), but only to establish a bandwidth parameter that essentially indicates how close observations need to be in order to be considered to arise from the same link. Given that the chain link dimensions are assumed to be known, this parameter becomes easy to adjust for the case at hand.

Thus, after applying mean shift to the multiple detections

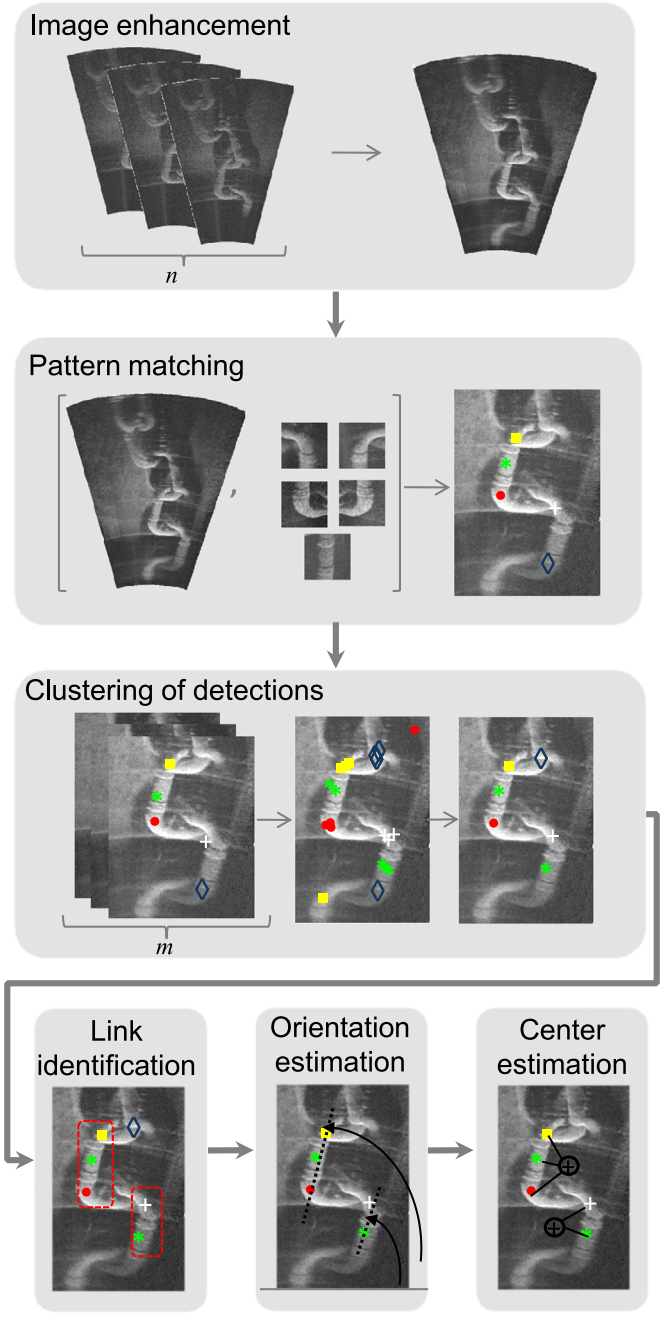

Fig. 4. Diagram of the link detection steps.

computed by the FLS detection module, the centroid of each of the determined clusters corresponds to the estimated link positions. These positions are then transformed to 3D waypoints which the vehicle will traverse to accomplish an accurate chain following.

Notice that this clustering approach solves implicitly the data association problem, i.e., determining to which link a new FLS detection corresponds, since on the arrival of each new detection the whole set of waypoints is recomputed according to the spatial layout of the link detections existing on the map. This strategy might seem inefficient as mean shift is known to be computationally expensive (Georgescu et al., 2003). However, for a two-dimensional feature space and taking into account that the number of detections accumulated during a chain-following procedure will not exceed the order of hundreds, its execution on the arrival of a new detection is entirely admissible. Notice also that thanks to the robust nature of the mean shift against outliers, the approach handles well any spurious detections that fall far from the link centres, thus avoiding the generation of erroneous waypoints and acting as a filter that updates the waypoint positions by seeking the highest detection support.

- **Sorting of link waypoints:** The output of the planner module at a given instant is the next waypoint that needs to be reached. Therefore, this module needs to maintain a list of ordered waypoints that refer to the centres of the detected chain links. Initially, the requested waypoint is the first on the list. When the vehicle reaches the desired location (considering a surrounding tolerance area) the requested waypoint will then change to the next one. This implies sorting the waypoints according to the distance with respect to the current vehicle position.

The described scheme (clustering in waypoints and sorting them) is periodically recomputed, meaning that the positions of the waypoints to follow are iteratively adjusted as more detections come in from the sonar detection module.

2.3. Vehicle guidance

Fig. 5 summarizes the workflow of a mission. The vehicle starts by executing a predefined survey trajectory over an area (e.g., a lawn-mower trajectory) while the detection module is running. If the survey ends without having detected any link the mission finishes reporting the chain not found. In case a link is detected during the survey, the chain-following is initiated, activating four concurrent actions (i.e., *Detect links*, *Compute Waypoints*, *Center last link in FoV* and *Follow link waypoints* in Fig. 5). On one side, the detection module keeps processing the incoming sonar images as has been described in Section 2.1 and the planner clusters the detections and determines the next link waypoint that the vehicle should visit. On the other side, there are two control actions that are performed concurrently in order to guide the vehicle through the waypoints dictated by the planner module while trying to keep the chain within the field of view of the sonar at all times. It must be noted that when the vehicle is over a waypoint, the sonar is inspecting an area located several meters ahead of the current vehicle position (depending on the configured range parameters). Thus, in

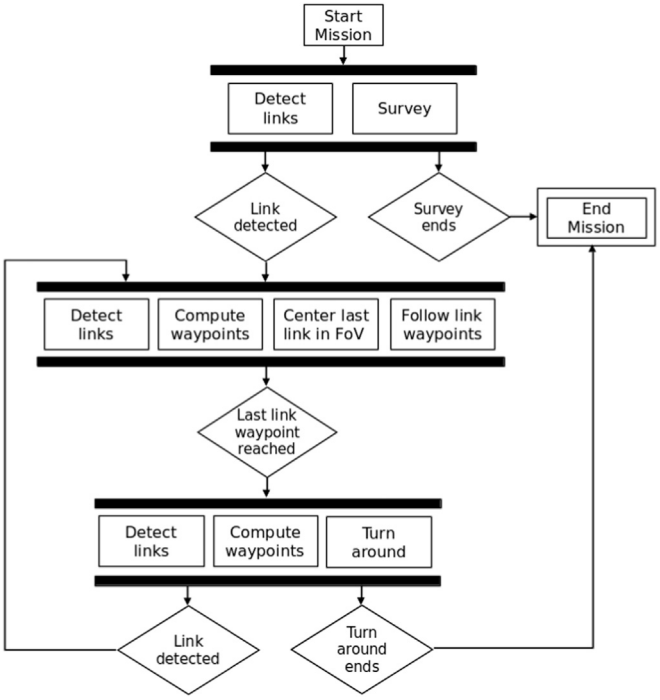

Fig. 5. Diagram of the mission workflow.

order to perform a seamless chain-following we need to maintain the chain within the field of view of the sonar, regardless of the vehicle position. To that end, our approach consists in a dual high level controller: on one side, a *xyz* position controller moves the vehicle to the desired waypoint coordinates. On the other, a yaw rate controller adjusts the vehicle's heading in order to keep the farther perceivable link waypoint in the middle of the sonar's field of view. The world coordinates of the link to be centred are transformed with respect to the mid point of the sonar's field of view. In this way, the error that must be compensated in order to keep the link in the middle of the image corresponds to the y coordinate of the obtained waypoint. By feeding this error to a proportional controller we obtain the velocity setpoint that will correct the yaw rate according to the link's distance to the center.

Given the imaging geometry of the sonar, a small variation on the vehicle's heading implies large movements in the sonar image plane, facilitating to maintain the link in sight. Moreover, the velocities requested to the *xyz* controller to move to a waypoint will be slow in order to facilitate the detections and therefore the velocity in which a link moves away from the image center will be from the same order. Hence, the yaw controller will be able to adjust the heading before the link drops off the field of view, provided that there are detections. With this strategy we ensure that we keep track of the farthest detected link as well as we increase the possibilities of detecting successive ones as the vehicle moves from waypoint to waypoint.

At a low-level, to fulfill the position or velocity requests, the AUV has two available control modes: pose (position + orientation) and twist (linear + angular velocities). A cascade control scheme is used to combine them. The pose controller, receives desired poses ($xyz\psi$) and transforms them into twist requests. It consists of a 4DoF proportional-integral-derivative (PID) controller. The second stage, the twist controller, receives desired twists ($uvwr$) and transforms them into wrench (force + torque) requests. It is composed of a 4DoF PID controller and a 4DoF open loop model working in parallel. Finally, the desired wrenches ($XYZN$) are transformed into thruster set-points by means of a thruster allocation matrix that distributes the desired wrench vector among the available thrusters according to their locations in the vehicle. It is worth pointing out that these low-level control scheme has been utilized successfully in the chain-following framework presented here, as will be shown in the experimental section. However, it is intended to be substituted for a robust controller with analytically guaranteed stability and convergence properties, in order to cope with the external disturbances that could create a cleaning water jet. The interested reader can find the analytical proofs and the full description together with preliminary results of the mentioned controller in Karras et al. (2014).

As can be seen in Fig. 5, a special situation occurs if the vehicle reaches the last waypoint and there are no links detected inside the sonar's field of view. This circumstance can take place when: a) the vehicle is arriving at the end of the chain and the links remaining to be visited are already too close to be inside the field of view or b) the chain presents a significant deviation in its trajectory and the links drop off the field of view before being robustly detected. If there are no detections, the controller can not adjust the heading accordingly and therefore it loses the track of successive links. In those cases the vehicle performs a *turn around* movement. It stops and rotates 45° left and right in order to look around for new links, which, in case of being found, are added to the planner list. The execution continues until the vehicle has reached the last waypoint in the list.

3. Vertical chain detection and following

In this section we consider a chain that is suspended in the water column, approximately in a vertical position (see Fig. 6). The location of a chain in such a configuration is *per se* a more difficult problem, as the seafloor does not constrain the search space and therefore the chain must be detected within a full 3D environment. Moreover, in this configuration, the chain can be subject to more motion than a chain resting on the seafloor. Given the narrow FLS field of view (both in elevation and azimuth angles) it is difficult to scan a 3D volume in an efficient way. For this reason, we make use of an auxiliary multibeam sensor to help in the initial chain localization phase. Hence, our approach for this scenario involves a multibeam sonar scanning in the horizontal plane (usually having a wider azimuthal field of view and longer operating range than the FLS), so that potential chain returns can be identified. From this point, the vehicle approaches the possible chain location and uses the FLS detection module explained in Section 2.1 in order to confirm the presence of the chain and initiate the following maneuver. It is important to note that in order to gather suitable FLS images to carry out this confirmation the sonar is set to a small grazing angle (~15°) with respect to the vertical plane. Fig. 7 shows a diagram summarizing the steps performed in this vertical scenario and each of the phases (detection, approaching and following) are detailed in the next sections.

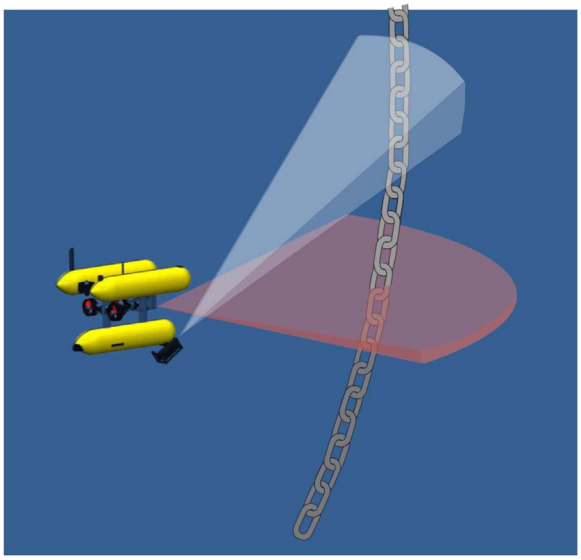

Fig. 6. Vertical chain scenario.

3.1. Detection of potential chain links in multibeam scans

As the vehicle navigates the environment the 3D range returns from the multibeam scans are projected onto the world frame. Incoming scans are accumulated in a short buffer, on a first input first output (FIFO), basis and the resulting point cloud is clustered into blobs at each time step. In order to discard spurious returns and other returns that might not conform to those of a chain link, several filters are applied over the accumulated point cloud map:

- **Minimum and maximum blob area**: blobs whose area is smaller than an established minimum will be rejected as spurious returns (e.g., returns from fish). Also, since the chain dimensions are known, we can neglect blobs that have a much larger area of that of a chain link.
- **Minimum and maximum distance**: a proper placement of the multibeam sonar in the vehicle should avoid noisy returns due to collisions with parts or structures of the vehicle's body. Nevertheless to prevent this potential flaw we discard the blobs that are within the first half meter of the current vehicle position. Similarly, blobs that are detected at greater distances, where the resolution of the multibeam with respect to the link dimension might be compromised, are also filtered out.
- **Minimum circularity**: the multibeam returns of a chain link

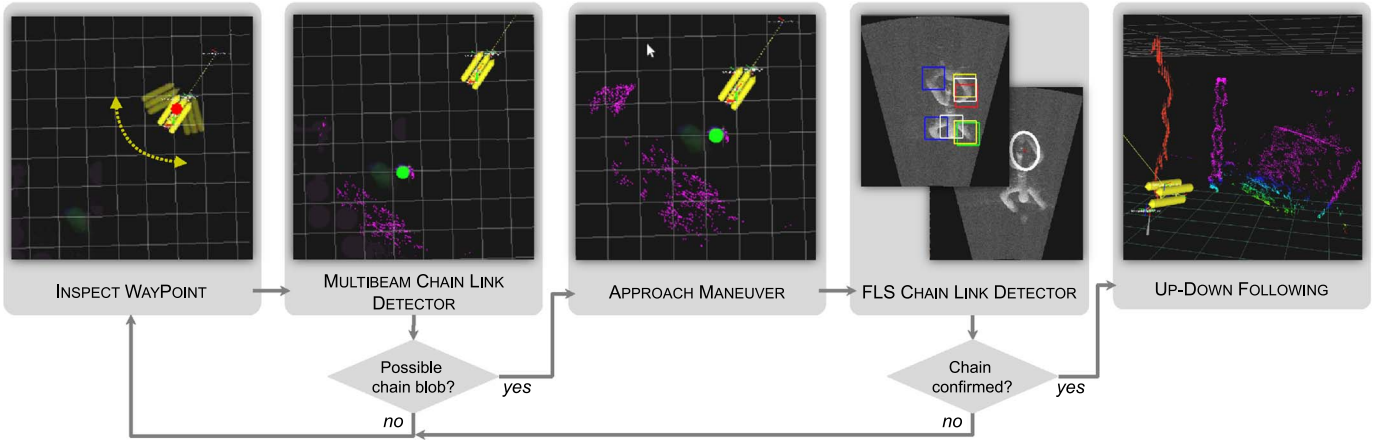

Fig. 7. Diagram of the chain following framework for the vertical scenario.

insonified from the horizontal plane are assumed to yield a roughly circular blob. Therefore, we impose a minimum circularity criterion so that possible elongated blobs (e.g., originating from a wall, a large structure, etc.) are discarded.

3.2. Approaching and confirmation of chain presence

After clustering and filtering the multibeam returns, if there is still a blob that can be considered a valid chain link candidate, the vehicle initiates an approaching maneuver. It navigates towards the potential chain position and stops at a given distance from the detected blob, keeping the heading towards it.

Because the position of blob detection can fluctuate due to noise in the detection process or because of the chain motion, the center of the detected blob is incorporated in an extended Kalman Filter (EKF) to obtain a better estimation. This filter stores in its state vector the vehicle position (x, y, z) and velocity (*surge*, *sway*, *heave*) as well as the blob center position (b_x, b_y, b_z). The EKF is not only updated by blob detections but also by any new measurement gathered by a navigation sensor, like the Doppler Velocity Log (DVL) or the depth sensor, using the orientation provided by the Inertial Motion Unit (IMU) as a control input. In this way, the drift accumulated during the approximation to the possible chain position is minimized.

Once in this position, using the same chain link detector described in Section 2.1, the system waits until it has received several link detections so as to confirm that the approached blob is indeed the chain. If that is the case, the following maneuver is triggered. Otherwise, if no confirmation of the presence of chain links is received, the vehicle proceeds to visit other chain candidates (if they exist) or else continues scanning the environment with the multibeam sonar.

3.3. Down-up following

Upon confirmation from the FLS detection module, the vehicle initiates the chain following maneuver. First, it moves down along the chain until reaching a predefined distance from the floor and afterwards it moves up until a given distance from the surface. Note that during this procedure the vehicle keeps a defined distance and orientation with respect to the currently detected blob, whose position is constantly updated in the 3D world map according to the incoming sonar data.

4. Experiments and results

In this section we present several experiments that have been conducted to validate the proposed framework. First, we introduce the experimental platform that has been used throughout the tests. Next we detail the experiments that have been performed in a controlled water tank environment to evaluate the performance of the chain link detectors, using the forward-looking and multibeam sonars. Finally, in an effort to assess the framework in a more realistic environment and conditions, we present the results of experiments carried out at sea, for both the horizontal and vertical scenarios.

4.1. Experimental platform

We tested the proposed framework using the Girona 500 AUV (Ribas et al., 2012), a reconfigurable, hovering-capable AUV actuated in 4 degrees of freedom (DOFs): Surge, Sway, Heave and Yaw. The vehicle is approximately 1 m by 1 m by 1.5 m length, weighing less than 200 kg. It is equipped with a complete navigation suite including a DVL, an attitude and heading reference system (AHRS), and a depth sensor. For the purpose of these experiments a SoundMetrics ARIS FLS (Aris explorer, 3000, 2016) and a Imagenex DeltaT multibeam were installed in the payload area. The ARIS FLS delivers high-resolution acoustic imagery, providing an angular resolution of 0.3° at the expense of having a narrow field of view (30°). The Imagenex DeltaT multibeam features 480 beams of 0.75° width spanning across its 120° swath aperture.

4.2. Chain link detection performance

The experiments described in this Section have been conducted in the water tank at *Center d'Investigació en Robòtica Submarina* (CIRS) of the University of Girona. To conduct the tests, we used a replica of a mooring chain consisting of 13 studless links measuring approximately 7 m in total. We evaluate first the performance of the FLS link detector described on Section 2.1 and then the link detection system used in the vertical scenario (which uses both multibeam and FLS data).

4.2.1. Detection on the horizontal scenario

To assess the performance of the FLS link detector the chain mock-up was deployed at the bottom of the tank (see Fig. 8). The sonar was mounted at a fixed tilt angle of 15 degrees throughout the experiments which is a suitable grazing angle for gathering images on the horizontal plane. The range window was set to 2.5 m, extending from 1 to 3.5 m ahead of the vehicle. Such short ranges were established with the aim of having a better image resolution and avoiding, at the same time, reflections from the tank walls.

According to the configured range samples, the acquired images (350×497 pixels) have a range resolution of 5 mm/pixel. The acquisition rate was set to 8 frames per second. At this frame rate, the detector module can generate an enhanced image every 3 frames and accumulate the individual template detections over 4 images, thus keeping the

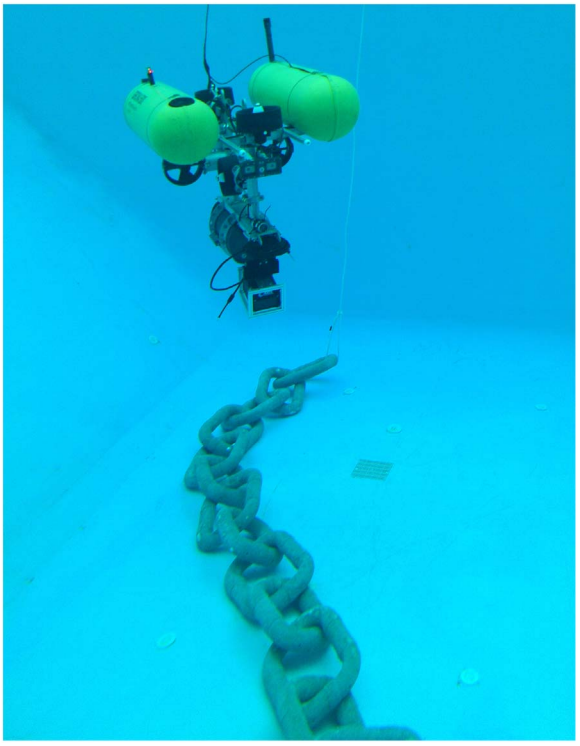

Fig. 8. Experimental setup at the University of Girona's water tank for the horizontal scenario: Girona 500 AUV equipped with the ARIS FLS and a chain mock-up deployed horizontally at the bottom.

processing in real-time and delivering link detections at 0.6 Hz.

It is worth pointing out here that there is a trade-off between these parameters and the speed of the vehicle. If the vehicle's speed is too high, the images would suffer significant appearance changes thus complicating the confirmation of new link detections as the vehicle moves forward. If no detections are performed this would cause the vehicle to stop and perform turn around movements more frequently, increasing the overall chain following time. If we reduce the template detections that we require in order to consider a detection valid (less than 4), we could increase the output frequency of the detector but that would decrease its reliability. Therefore, the only option for increasing the speed would be to increase the sonar frame rate. The frames per second (fps) of the FLS can be increased, however the detection algorithm is not able to process more than 8 fps with the available vehicle's processing power and that slows down the detection step as well as subsequent steps. We have seen that with the current frame rate employed (8 fps) the full framework can work reliably with the vehicle moving at 0.1 m/s. Note that this is enough to perform the following of a chain lying horizontally on the floor (which would be always rather static) but it could be a bottleneck in trying to follow the chain faster or following a chain that is affected by considerable motion.

To start the experiment, the vehicle was tele-operated near one of the chain ends and was left in a position where some chain links could be seen. From then on, the described framework took control of the vehicle to drive it autonomously over the chain. Note that to evaluate the performance of the detector we could have tele-operated the vehicle over the chain, however we decided to execute the full framework so that the images are gathered in the actual operating conditions, thus not favoring or influencing factors such as the vantage point or the vehicle speed.

As the vehicle was set to move at a low speed (0.1 m/s), many of the links were in the sonar's field of view for enough time to be detected on multiple occasions. During the course of traversing the chain the detector produced a total of 376 detections, effectively detecting 10 different chain links. In order to evaluate the accuracy of the link detector independently of potential errors introduced in the two subsequent modules, we have manually labelled the link center on those images where a link was detected. Table 2 summarizes the number of times that each of the 13 links were detected, together with the mean error computed with respect to the manually labelled center.

Table 2
Table showing the number and accuracy (compared to manually labelled link centres) of the link detections along the chain following experiment.

Link number	Link detections	Mean error (cm)	Link number	Link detections	Mean error (cm)
1	0	–	8	33	4.5 ± 3.9
2	0	–	9	83	7.9 ± 9.5
3	0	–	10	23	6.8 ± 14.1
4	22	12.3 ± 3.6	11	30	10.2 ± 13.3
5	12	6.5 ± 9.2	12	21	9.9 ± 5.9
6	5	7.2 ± 5.1	13	122	5.6 ± 16.3
7	25	4.8 ± 4.7			

Note that the first 3 links were never detected. This is due to the limited space in the test tank that did not allow for the necessary distance between the vehicle's starting position and the first chain links to be detected. The rest of the links were detected multiple times, depending on how much time they were in the sonar's field of view and how well they were observed. Regarding the accuracy, all link centres have an estimated error below 15 cm. These errors are due to the variability of the template matching step as well as the assumption of the 2D projection when determining the link centres. Relatively to the link size, they are all below 1/4 of the link's length and therefore we can consider that we achieve an acceptable detection accuracy to perform the chain-following.

4.2.2. Detection in vertical scenario

To validate the detection of the chain in the vertical configuration, we conducted several tests in the CIRS water tank, this time hanging the chain replica vertically from a crane (see Fig. 9). The multibeam sonar was configured at 10 m range and delivered a full 120 swath comprising 480 points at 10 Hz. The blob detection algorithm was set to a buffer size of 10 in order to accumulate enough points to form blobs and then perform the filtering to discern which ones are potential chain returns. Therefore the map of detected blobs was updated each second. Smaller buffers would increase the risk of clustering blobs of non-significant returns (and trigger too many hypotheses to inspect) while a too large buffer would have a negative impact on the speed of the system. Table 3 summarizes the parameters that were set for the experiment.

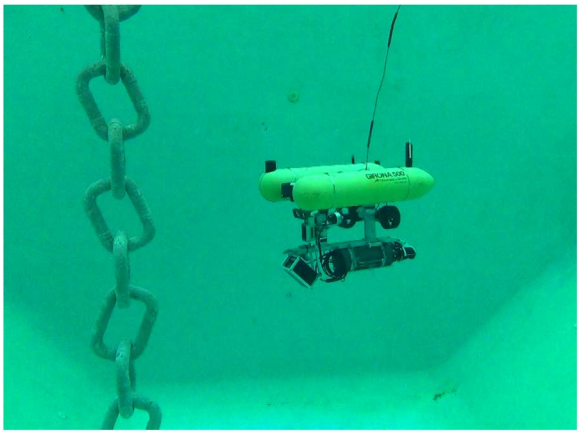

Fig. 9. Experimental setup at the University of Girona's water tank for the vertical scenario: Girona 500 AUV equipped with the Imagenex multibeam sonar and the ARIS FLS and the chain mock-up suspended vertically.

Table 3
Parameters used in the multibeam detection.

Parameter	Value
Multibeam Range	10 m
Point Cloud Buffer size	10
Minimum Distance	0.5 m
Maximum Distance	4.5 m
Minimum Circularity	0.6
Maximum Circularity	1
Minimum Area	0.0225 m^2
Maximum Area	0.16 m^2

Table 4
Summary of detector performance tests on vertical chain.

	Chain	Chain & buoy	Buoy	Empty tank
No. of detected chain hypothesis	5	11	5	1
No. of confirmed chain presence	5	5	0	0

We have performed 5 executions in 4 different configurations changing the objects placed in the water tank as follows: only the chain; the chain together with another object (submerged buoy); only with the buoy and finally without anything inside the tank. Table 4 summarizes for each case how many chain hypothesis have been detected with the multibeam and how many have been confirmed as a true chain link using the FLS detection algorithm. In each of the 5 executions the vehicle started at a different distance from the chain (ranging between 1 and 5 m as the water tank space did not allow for larger distances), and from different angles within the 120° multibeam FoV.

In the first 5 executions, only the chain mock-up was deployed in the tank. Despite the presence of the wall returns and other scattered multibeam points, the detector was always able to identify a chain blob thanks to the different applied filters (sizes, circularity, etc.). When approaching the detected chain position, the FLS detection module always confirmed the presence of a link.

We then introduced a submerged buoy of similar dimensions to those of a chain link, so that we forced the appearance of more blobs in the multibeam image. In these executions, two possible chain blobs were detected among the multibeam returns, and the vehicle approached first the one located closer. When that was the buoy, the FLS link detector did not trigger a valid confirmation and after the set timeout, it continued to inspect the other blob.

Finally we observed that in case of removing the chain from the tank the detector generally does not output any link hypothesis, even though as said previously, there are several returns from the tank walls. In one of these attempts a blob had been detected out of some returns from another vehicle moving in the water tank but, as expected, when reaching the blob position it did not receive confirmation of a link presence with the FLS. Therefore, the combination of the two detectors allows us to reliably identify the presence of the chain in the water column.

It is worth emphasizing that the accuracy of the detection depends on the resolution of the employed multibeam sonar, the chain dimensions and the distance from which the chain is insonified. With the beam width of the employed multibeam (0.25°) observing the chain from 10 m we have a resolution of approximately 5 cm which warrants a considerable number of returns on the employed mock-up links (which are around 40 cm wide) and therefore a good detection accuracy. For the same chain size, if the vehicle is located more than 30 m apart from the chain that will reduce considerably the number of returns and also the accuracy as the beam resolution will quickly decrease at around 13 cm. However, notice that once a chain blob has been confirmed by the FLS detector, the accuracy of the link detection in the following maneuver is high as the vehicle maintains a close distance with respect to the chain.

Fig. 10. Map of the experimental site in Sant Feliu de Guixols harbor. The red square shows the area where the tests took places.

4.3. Chain following and mapping performance

In order to test the full framework -including chain detection, following and mapping- under more realistic conditions, we conducted trials in the harbor of Sant Feliu de Guixols, located on the coast nearby Girona (Catalunya, Spain), see Fig. 10. The chain mock-up was deployed in the area with the help of a diver and Girona 500 AUV was deployed from the University of Girona's boat. During all the experiments the vehicle operated in fully autonomous mode, being connected only to a surface buoy in order to have real-time feedback of the mission state. In addition to the already described sensors, the vehicle was equipped with two video cameras in order to have other perspectives of the course of the experiments if visibility allowed. Even though the operating area was protected by the harbor breakwater the operating conditions were rough due to strong winds that persisted all the week. Underwater visibility varied during this period from 1 to 5 m.

Next sections describe the experiments and results obtained in the two scenarios. For a more visual account, two video files showing the course of action of the horizontal and vertical experiments conducted at sea can be found together with the electronic version of this manuscript.

4.3.1. Horizontal scenario

In order to test the framework in the horizontal scenario, the chain mock-up was placed laying on the sea bottom, at approximately 15 m depth (see Fig. 11). In order to conduct the chain search, a lawnmower trajectory was defined in the vicinity of the chain position (since its approximated position is assumed to be known). Fig. 12 shows an example of one search trajectory that was performed around 1.5 m altitude. The vehicle surveyed 5 transects without detecting any link. On the way to the 6th waypoint, the FLS detector output a link detection and the chain following algorithm was initiated. In this case, the vehicle detected a chain link from an extreme end of the chain and the rest of the links were detected sequentially, completing the following until the other chain end. In the last part of the trajectory, since the last chain links were already too close to be seen by the FLS, the vehicle performed some turn-around movements to look for links out of sight, but since none were seen it simply continued following the waypoints until the last detected one.

Fig. 12 also depicts the AUV trajectory (in blue) and the link detections (in green) plotted on the world frame, together with the waypoints (in red) that the trajectory planner module has associated to

Fig. 11. Chain deployment in Sant Feliu harbor for the horizontal scenario.

the detections. Fig. 13 shows a close up of the area where the chain following was performed. It is important to remark that the link waypoints are dynamically recomputed during the whole experiment as new detections appear by following the procedure described in Section 2.2, thus the depicted link waypoints in the figures are the last estimation for each link. Since the test chain was short, when the vehicle reached the middle of the chain the farthest links were no longer visible, thus triggering the turn around movement at each of the remaining waypoints. The online adjustments in the position of the waypoints together with the small vehicle displacements induced from the turn around movements explain the slightly jagged trajectory of the AUV. It is also worth noting that a distance threshold of 0.3 m was used when judging whether the vehicle had arrived to a waypoint. For this reason, the AUV trajectory does not go over the exact position of the link waypoints but effectively passes through this 0.3 m tolerance radius.

Hence, we can see that the vehicle was driven successfully through the sequence of waypoints, but to evaluate the performance of the trajectory planner module we must ensure that the scattered detections have been correctly associated to the different links, or in other words, we must verify that the performed trajectory went over the actual chain links. To conduct such verification we would require the ground truth positions of each link in the environment, which unfortunately are not available. As an alternative, we compare the estimated link waypoints of the trajectory against an acoustic mosaic of the acquired FLS images during the experiment. The mosaic is referenced with respect to the first sonar frame and therefore can also be referenced in world coordinates by using the vehicle location where the first frame was gathered. To build such a mosaic we compute the pairwise registration of each frame with a window of frames in its neighborhood using Fourier-based techniques (Hurtós et al., 2015). All the obtained pose constraints are then fed into a pose-based graph optimization, that leads to the maximum likelihood configuration of the sonar images. Finally, the frames can be fused by averaging the pixel intensities at each location. The obtained mosaic is visually consistent, indicating that the registration of the frames has been successful. Fig. 14 shows the link waypoints overlaid on the acoustic mosaic. As can be seen, the computed link waypoints closely follow the chain links thus testifying to the accuracy of our chain following scheme. Although there were some outlier detections (see some isolated detections in Fig. 13), they neither yielded outlier waypoints nor affected the position of the computed ones thanks to the filtering performed by the planner module. We can see that most of the waypoints have been correctly associated to an actual chain link, except for the 4th and 5th links where the trajectory planner determined the presence of only one link waypoint. Indeed, if we look at Fig. 13 we can see that the detections around this waypoint are highly scattered. Probably this is because the 4th link was interlaced with its neighbours in a way that caused it be tilted and more elevated, thus making its detection more difficult. Hence, the trajectory planner has merged the few detections of this 4th link with those of the 5th, leading to a sole waypoint placed in the middle of the two actual links. Nevertheless, this did not affect the chain following as the waypoint was indeed over the chain.

Although in this case the trajectory that was defined to search for the chain did not allow for a full coverage of the area (the transects were more spaced than the sonar's field of view), the mosaic of Fig. 14 also testifies to the capability of the framework for mapping the chain and its surrounding area. At this point it is worth adding a note on the resolution that we can achieve with these kinds of maps. The actual resolution in which a mosaic is rendered is, by default, the same as that of a single frame. In this sense, a frame and a corresponding mosaic covering the same area will have the same number of pixels, which will

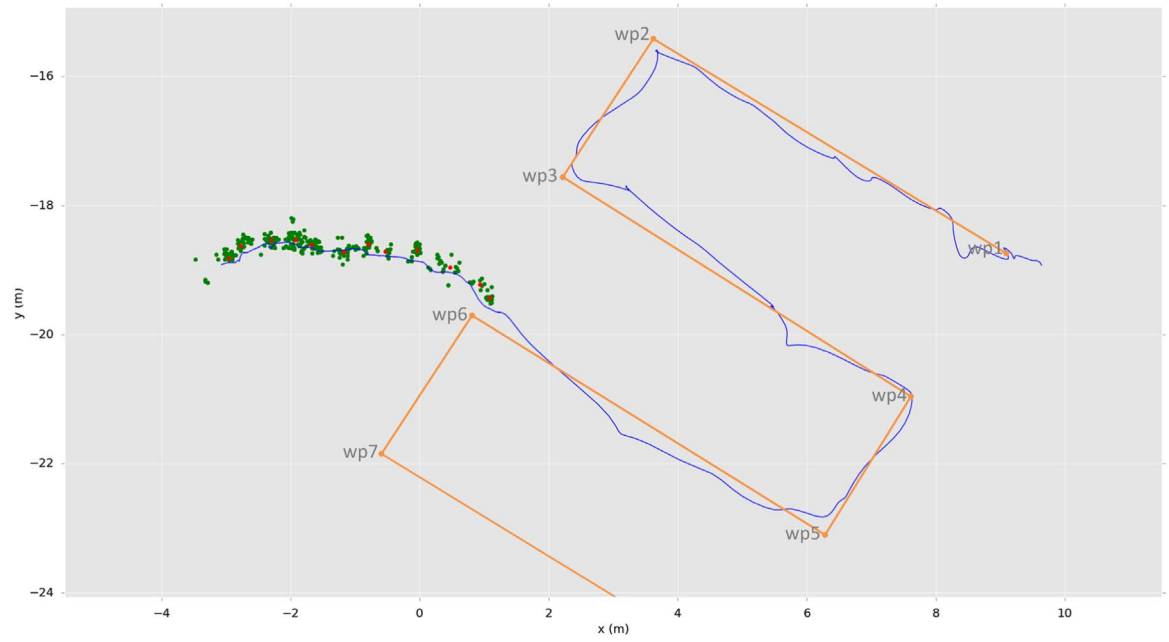

Fig. 12. AUV trajectory along the chain following experiment (in blue). Green dots show the multiple link detections from the FLS detector while red ones show the estimated link waypoints computed by the planner. (For interpretation of the references to color in this figure legend, the reader is referred to the web version of this article.)

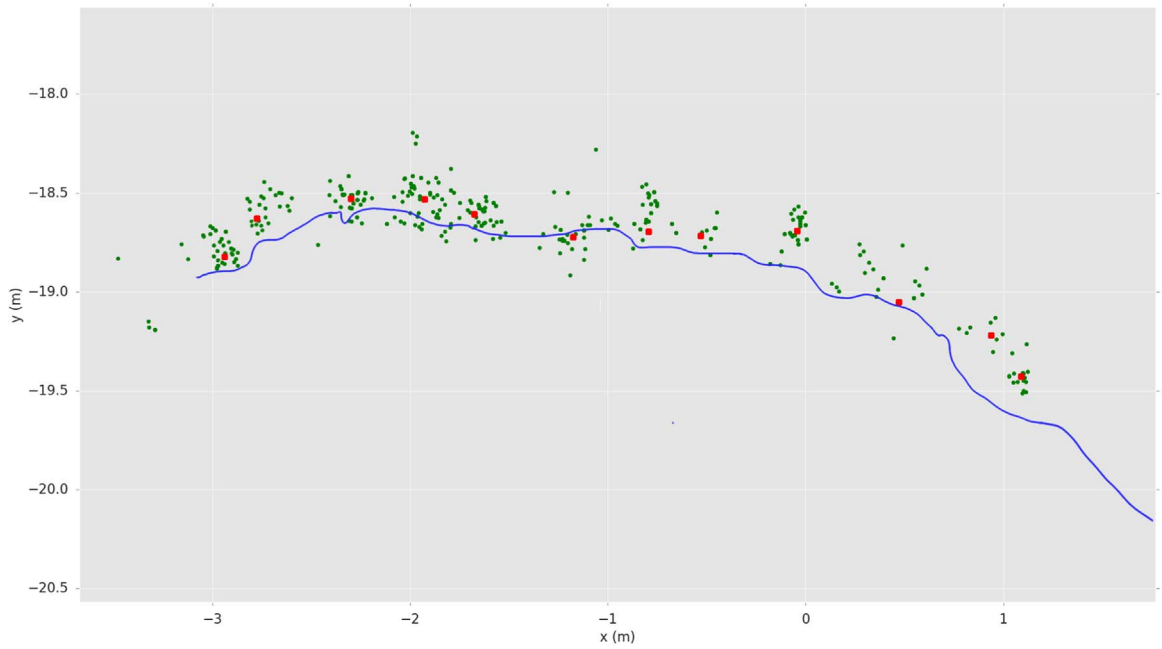

Fig. 13. Close up of the AUV trajectory during chain following. In green: individual link detections. In red: waypoints computed by the planner module. (For interpretation of the references to color in this figure legend, the reader is referred to the web version of this article.)

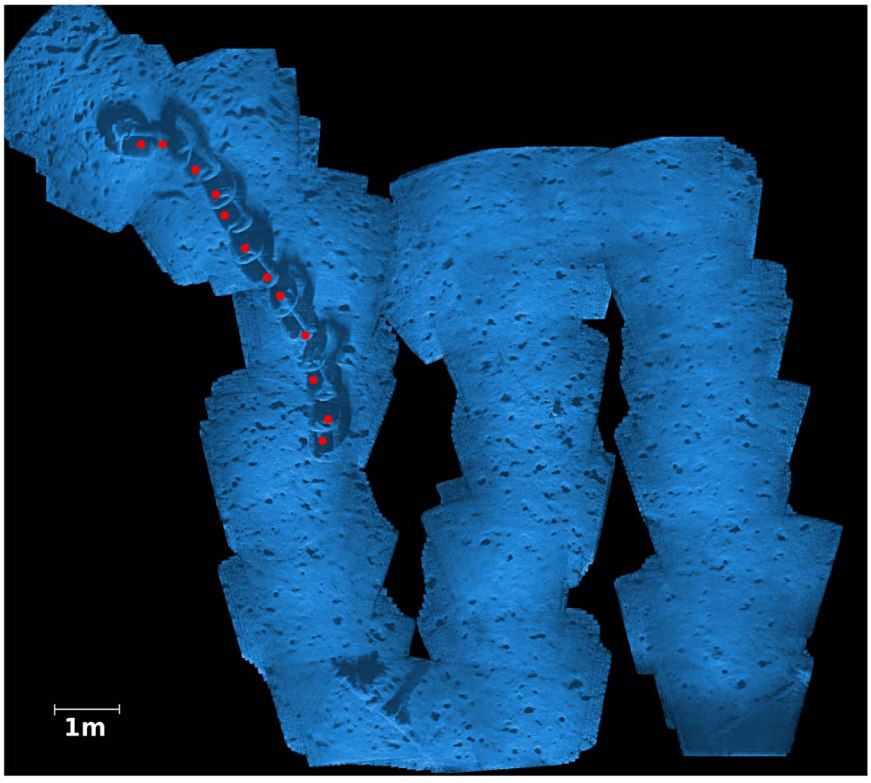

Fig. 14. Acoustic mosaic generated by registering the acquired sonar frames along the vehicle trajectory with the link waypoints overlaid in red. Note how the link waypoints closely follow the actual link locations.

be determined by the sonar resolution (based on the sonar characteristics and the configured range and number of beams). For instance, for the Sound Metrics ARIS sonar that we have used the theoretical maximum resolution according to the device specifications is 3 mm. However, a single FLS image has a much lower apparent resolution, as a consequence of the inhomogenous mapping from polar to Cartesian coordinates that assigns the same pixel intensity to several pixels in the Cartesian domain. In the mosaic, this effect is attenuated as a consequence of the averaging of multiple frames, thus leading to an improvement of both apparent resolution and signal-to-noise ratio. In addition, the real resolution can be indeed increased thanks to the mosaicing process. We can take advantage of the multiple alignment of low-resolution images together with the sub-pixel accuracy positions obtained from the global alignment step to perform super-resolution. By oversampling the mosaic grid and mapping the images with sub-pixel transformations, we achieve a higher resolution and an overall

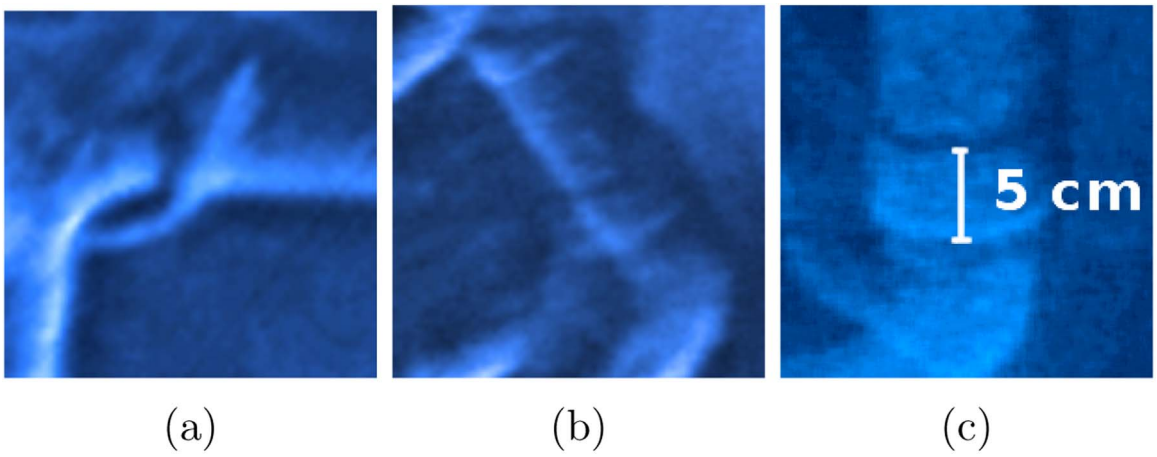

Fig. 15. Three different close-up details of the rendered mosaic, showing a rope and some link features at centimetre-level.

enhancement of the mosaic image. The mosaic presented in Fig. 14 has a resolution of 4.5 mm/pixel. Fig. 15, shows some close up details of the mosaic. Note how features of few centimetres on the chain links can be clearly identified.

Thus, although the precision of the measures will always be heavily conditioned by the imaged scene configuration as well as the insonified material, the rendered mosaic proves useful to have a preliminary map of the chain state and its spatial layout in the environment. It is worth underlying though, that in order to perform a thorough inspection that conforms to the requirements of the main regulators in the field (which require millimetre precision measurements) (DNV Offshore Mooring Chain Standard, 2016), data should be extracted with other inspection techniques.

Overall, the results of horizontal chain-following at sea were positive, confirming the performance observed in the water tank despite the more challenging conditions for vehicle control and demonstrating the ability to detect the chain within a much larger environment and follow it accurately.

4.3.2. Vertical scenario

In this section, we present the results obtained in the harbor tests for the vertical scenario. For this set of experiments, the chain mock-up was hung vertically from a floating container at the surface. Since the deployment area was around 15 m deep the chain links ended at approximately 2 m above the seafloor. Similarly to the horizontal scenario, in order to test the vertical chain detection several waypoints were automatically defined in the vicinity of the chain position. In each waypoint, the vehicle was set to perform a 360º turn so as to inspect all directions. The multibeam sonar was configured to shoot at 20 m range, and the detector was set to accumulate 10 range scans to cluster the multibeam returns in blobs of possible chain locations. The rest of the parameters were set to the same values shown in Table 3.

During the multiple tests, the multibeam detector did not fail to identify the presence of the chain blob within the environment. Indeed, operating in a large, open environment helped to achieve a better performance in comparison with the water tank tests, as the actual chain blob was the only hypothesis of chain that was consistently found in every run. Returns from the harbor's walls were duly discarded as well as some spurious returns from nearby mooring ropes, which raised some points in the map, but not enough to be considered link detections according to the established blob area size criteria.

Fig. 16 shows an example of one approximation to the chain from the inspection waypoint at which it was detected. When approaching the detected chain position, the FLS detection module was able to confirm the presence of a link (see Fig. 17) and therefore the following maneuver (down-up) was triggered. During that, the multibeam detector always made a good estimation of the chain links and remained oriented towards them while maintaining a constant distance. Fig. 18 shows an example of the data from one of the chain-following maneuvers performed at sea. We can see how after correctly performing the chain following the accumulated multibeam point cloud describes the shape of the chain (see Fig. 18(a)). Fig. 18(b) shows the acoustic mosaic built from the FLS frames, using the procedure previously explained for the horizontal case. Finally, since the vehicle was keeping a close distance to the chain (1 m) and the visibility during the tests was fairly good, the images from the vehicle's stereo camera also allowed to perform a 3D reconstruction of the chain (see Fig. 18(c)).

Since in the vertical scenario it is more likely that the chain undergoes some motion, it is worth adding a note on the framework's performance under these circumstances. It must be noted that during the following maneuver the chain is already located and only minor position corrections are required to keep the vehicle oriented and at a constant distance from the multibeam detections. Moreover, thanks to the large field of view of the multibeam and its fast update rate (10 Hz), it is more difficult to lose the chain returns and therefore there is no need for turn-around movements. All this facilitates the following maneuver at a faster vehicle speed than in the horizontal case, approximately at 0.2 m/s. Hence, the current framework is resilient to small chain motions as the multibeam sonar is fast enough to concentrate sufficient points at the actual chain location, update a detection hypothesis accordingly, and keep it inside the filter to correct the vehicle pose.

However, if the chain motion is large the beam returns would become too spread, leading to them being possibly discarded and therefore the pose of the chain could not be reliably estimated. Besides, even though the detections were accurate, the dynamics of the AUV are generally slow and would be difficult to follow them accurately.

In order to cope with these issues we envisage two possible solutions. On one hand, we could try to increase the speed of the system (e.g., by using a multibeam with higher update rate or increasing the vehicle's control loop) and try to perform the following maneuver with the vehicle being perpendicular to the main chain motion axis. In this way, the majority of required control actions would be targeted to correct the vehicle's heading, providing two major advantages: the heading is the DOF that allows to keep facing the chain with less movement while it is also the faster and more controllable DOF of the AUV (with a dedicated sensor for its measurement). Another possible option to improve the behaviour of the system under significant chain motion, would be to modify the EKF filter. Instead of considering a static chain model we could use a motion model more close to that of a swinging chain. This would allow to

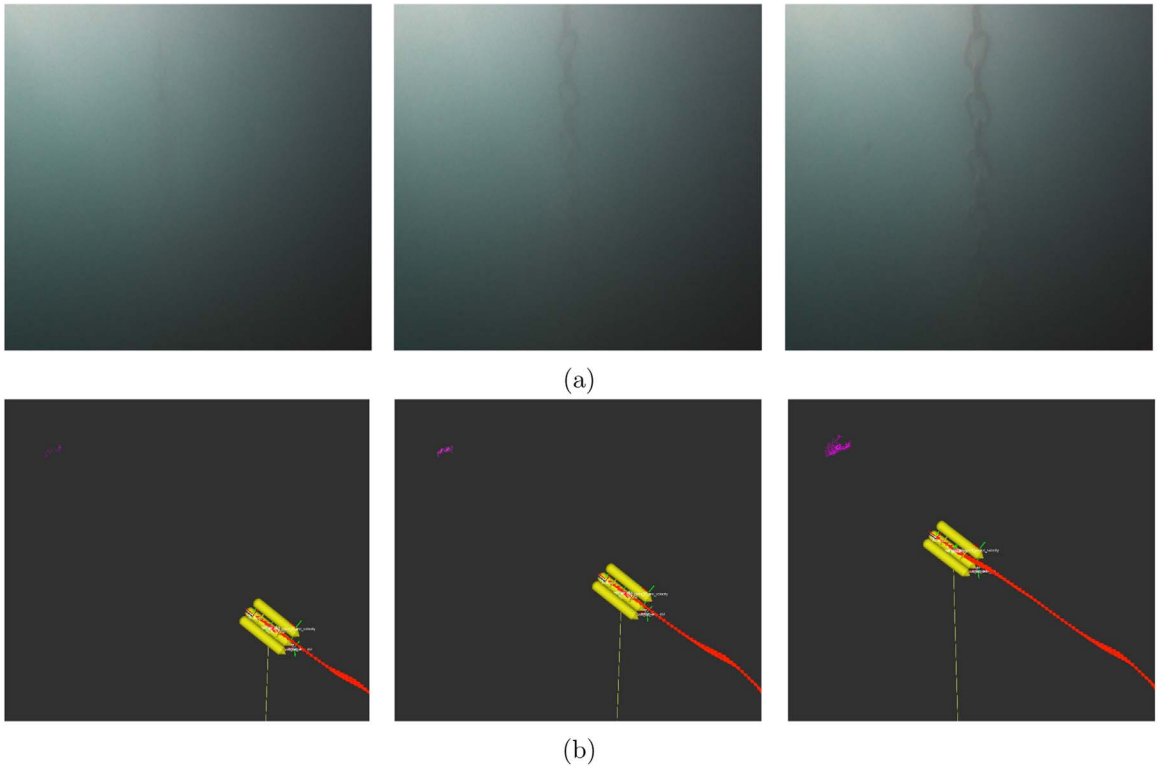

Fig. 16. Approximation from the inspection waypoint to the chain position. a) View from the optical camera. b) Map of the multibeam scans. At the time when the leftmost images were taken, the detection of a possible chain location was performed through the multibeam data whereas it would have been difficult to do so from the camera image.

predict the chain position in a better way and therefore adjust the vehicle control, leading to a smoother following maneuver.

Regarding the mapping, if there is significant chain motion the images will be gathered from significantly different vantage points. As the forward-looking sonar is sensitive to the viewpoint changes the mosaicing system will most likely fail to produce a consistent map as the differences in appearance along the trajectory would complicate the registration between frames. Indeed, some blurring can be already be perceived in the mosaic of Fig. 18(b) due to small motions of the chain. Therefore, in case of considerable motion, a preliminary inspection of the chain state could only be done by checking out the individual gathered images instead of the mosaic. This would complicate the perception of the chain's spatial arrangement as well as losing advantages such as the increased SNR and resolution that the mosaic offers.

5. Conclusions and future work

This paper has presented an autonomous system that integrates sonar perception, planning and control disciplines, as a first step towards achieving autonomous cleaning and inspection of underwater mooring chains. The problem has been tackled using sonar as the main perception sensor so as to enable the operation in turbid water conditions. We have dealt with two separate scenarios: horizontal (with the chain lying on the seabed) and vertical (with the chain hanging in the water column).

We have proposed an algorithm that exploits the sonar's high frame rate and applies local pattern-matching to handle the complexity of detecting link chains in acoustic images. Experiments in a water tank have shown that the developed algorithm can identify the position of the chain links in the acoustic images with an error of a few centimetres. After the detection, an approach based on a k-means

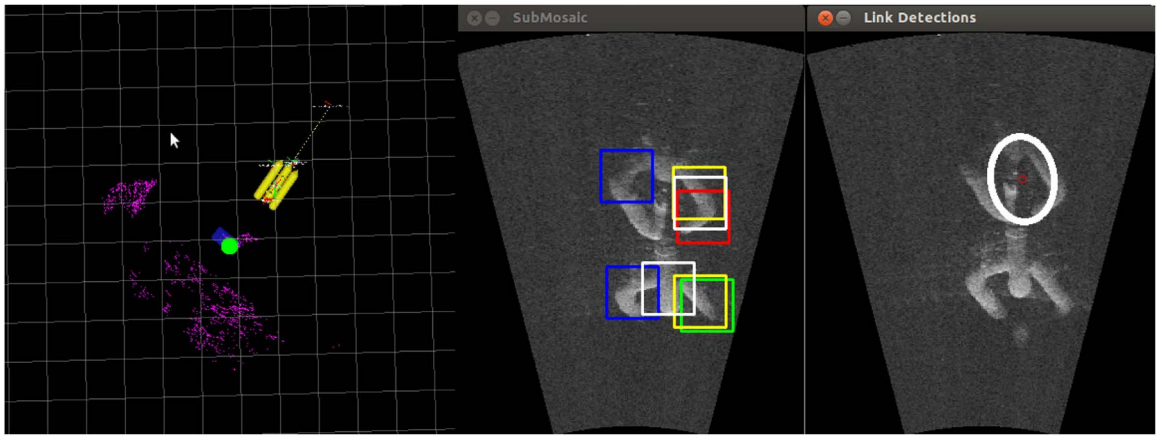

Fig. 17. Confirmation of the chain presence. Snapshot of the instant when the vehicle has approached the potential chain position and confirms the chain presence using the FLS link detector.

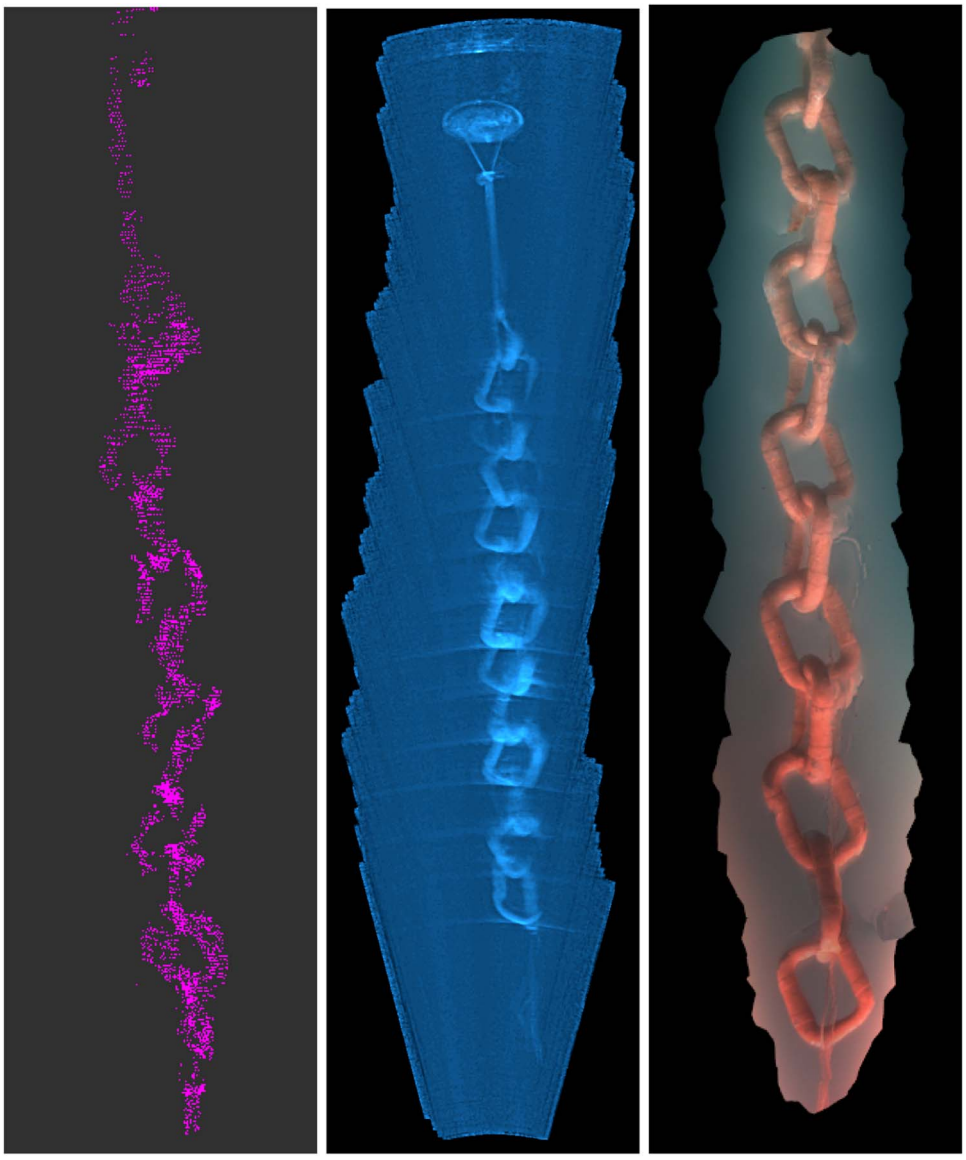

Fig. 18. Data from a vertical following maneuver at sea. a) Accumulated multibeam point cloud. b) Acoustic mosaic generated by registering the acquired FLS frames. c) 3D reconstruction from the vehicle's stereo camera.

clustering is used to associate the multiple detections with the corresponding link waypoints and build the trajectory along the chain. Then, the vehicle is guided through these waypoints using a high level controller that has been tailored to simultaneously traverse the chain while keeping track of upcoming links. In the vertical scenario, the FLS detector has been complemented with a multibeam detection algorithm so that the multibeam data is used to identify potential chain returns from far distances, keeping the hypothesis as features inside an EKF filter. The FLS detector is used to confirm whether the detected hypotheses are indeed from a chain and finally the vehicle is commanded to move along the chain maintaining distance and orientation to the constantly updating multibeam detections.

Experiments in a harbor environment have been conducted to validate the performance of the system in finding, following and mapping a chain in both scenarios. The framework proved able to locate the chain within a much larger and unconfined environment. The visual consistency of the visited waypoints on a mosaic generated by registering the acquired frames, has demonstrated that the vehicle is able to perform a trajectory closely following the link's centres. Furthermore, the resolution of the obtained acoustic mosaics allows identification of features down to centimetre level thus providing a useful map for detecting chain parts that need further cleaning or inspection.

Future work will be directed towards increasing the technology readiness level (TRL) of the system, making an effort to bring it more close to a real scenario. In this line, we will perform the installation of a pan and tilt unit to be able to modify the FLS tilt angle during operation and implement the transition from the horizontal to the vertical scenario. We will also explore the suggested improvements to be able to cope with larger chain motion as well as conduct tests under a more realistic setup (i.e., full scale chain, buried sections, etc). Another future development concerns the integration of a water jet and a new low-level controller, which has already been developed and tested (Karras et al., 2014), to follow the chain while compensating accordingly for the force/torque disturbances produced by the jet.

Finally, we would like to mention that although the work presented here focuses on underwater chain following and mapping, we believe that by further developing the involved disciplines (sonar detection,

planning and control) the system can become more widely applicable. For instance it could contribute to the assessment of other structures such as pipelines or harbor infrastructures where visibility conditions typically restrict the use of optical inspection methods.

Acknowledgments

This work was supported by the EU funded project PANDORA: Persistent Autonomy through learNing, aDaptation, Observation and ReplAnning", ref. FP7-288273.

Appendix A. Supplementary data

Supplementary data associated with this article can be found in the online version at http://dx.doi.org/10.1016/j.oceaneng.2016.11.072.

References

Aris explorer 3000, 2016. retrieved May 2016, from ⟨http://www.soundmetrics.com/Products/ARIS-Sonars/⟩.

Comaniciu, D., Meer, P., 2002. Mean shift: a robust approach toward feature space analysis. IEEE Trans. Pattern Anal. Mach. Intell. 24 (5), 603–619.

DNV Offshore Mooring Chain Standard. 2016. retrieved May 2016, from ⟨https://rules.dnvgl.com/docs/pdf/DNV/codes/docs/2013-10/OS-E302.pdf⟩.

Ferreira, F., Djapic, V., Micheli, M., Caccia, M., 2014. Improving automatic target recognition with forward looking sonar mosaics. IFAC Proc. Vol. 47 (3), 3382–3387.

Galceran, E., Djapic, V., Carreras, M., Williams, D.P., 2012. A real-time underwater object detection algorithm for multi-beam forward looking sonar. IFAC Proc. Vol. 45 (5), 306–311.

Georgescu, B., Shimshoni, I., Meer, P., 2003. Mean shift based clustering in high dimensions: A texture classification example. In: Computer Vision, 2003. In: Proceedings of the Ninth IEEE International Conference on, IEEE, pp. 456–463.

Hall, A., 2005. Cost effective mooring integrity management. In: Offshore Technology Conference.

Handegard, N.O., Williams, K., 2008. Automated tracking of fish in trawls using the didson (dual frequency identification sonar). ICES J. Mar. Sci.: J. du Cons. 65 (4), 636–644.

Hurtós, N., Ribas, D., Cufí, X., Petillot, Y., Salvi, J., 2015. Fourier-based registration for robust forward-looking sonar mosaicing in low-visibility underwater environments. J. Field Robot. 32 (1), 123–151.

Hurtos, N., Nagappa, S., Cufi, X., Petillot, Y., Salvi, J., 2013. Evaluation of registration methods on two-dimensional forward-looking sonar imagery. In: OCEANS'13 MTS/IEEE.

Hurtos, N., Palomeras, N., Carrera, A., Carreras, M., Bechlioulis, C.P., Karras, G.C., Hesmati-alamdari, S., Kyriakopoulos, K., 2014. Sonar-based chain following using an autonomous underwater vehicle. In: 2014 IEEE/RSJ International Conference on Intelligent Robots and Systems, IEEE, pp. 1978–1983.

Hurtós, N., Palomeras, N., Nagappa, S., Salvi, J., 2013. Automatic detection of underwater chain links using a forward-looking sonar. In: OCEANS-Bergen, 2013 MTS/IEEE, IEEE, pp. 1–7.

Karras, G.C., Bechlioulis, C.P., Nagappa, S., Palomeras, N., Kyriakopoulos, K.J., Carreras, M., 2014. Motion control for autonomous underwater vehicles: A robust model-free approach. In: 2014 IEEE International Conference on Robotics and Automation (ICRA), pp. 6529–6534.

Morandini, C., Legerstee, F., Consistent integrity of mooring systems, ISOPE, Osaka, Japan.

Noble Denton Europe Limited, 2006. Research report 444 floating production system. Tech. rep., Health and Safety Executive (HSE).

PANDORA: Persistent autonomy through learning adaptation and re-planning, 2016. retrieved May 2016, from ⟨http://www.persistentautonomy.com⟩.

Petillot, Y., Ruiz, I.T., Lane, D.M., 2001. Underwater vehicle obstacle avoidance and path planning using a multi-beam forward looking sonar. IEEE J. Ocean. Eng. 26 (2), 240–251.

Quidu, I., Jaulin, L., Bertholom, A., Dupas, Y., 2012. Robust multitarget tracking in forward-looking sonar image sequences using navigational data. IEEE J. Ocean. Eng. 37 (3), 417–430.

Reece Innovation, 2016. retrieved May 2016, from ⟨http://www.reeceinnovation.com/work/crawlers-for-cleaning-inspecting-pipelines-and-mooring-chains/⟩.

Reed, S., Petillot, Y., Bell, J., 2004. Automated approach to classification of mine-like objects in sidescan sonar using highlight and shadow information. IEE, Proc.-Radar Sonar Navig. 151 (1), 48–56.

Reeves, T., Mcleod, D., Embry, C., Nickerson, B., et al., 2014. Auv-based 3d laser inspection for structural integrity management in deepwater fields. In: Offshore Technology Conference, Offshore Technology Conference.

Ribas, D., Palomeras, N., Ridao, P., Carreras, M., Mallios, A., 2012. Girona 500 auv: from survey to intervention. IEEE/ASME Trans. Mechatron. 17 (1), 46–53.

Sawas, J., Petillot, Y., Pailhas, Y., 2010. Cascade of boosted classifiers for rapid detection of underwater objects. In: ECUA 2010 Istanbul Conference. pp. 1–8.

Welaptega Marine Limited, 2016. retrieved May 2016, from ⟨http://www.welaptega.com/chain-measurement-methods-pros-and-cons/⟩.

Xie, S., Chen, J., Luo, J., Xie, P., Tang, W., 2012. Detection and tracking of underwater object based on forward-scan sonar. In: International Conference on Intelligent Robotics and Applications, Springer, pp. 341–347.